Mediterranean Forests in Transition (MEDIT): Deliverable No4

Title: Report on the development of the DGVMs

Due to Project Month 20, Date: 30/11/2013

Introduction

This report presents the evaluation of an existing Dynamic Global Vegetation Models (DGVMs) under Mediterranean climatic conditions and vegetation characteristics, and the developments made to a hybrid model in order to be applicable to Mediterranean and Mountainous Mediterranean Forests, both at the local and the regional scales. These activities are based on the use of data gathered in MEDIT's project Working Package 4. Although the data assimilation Work Package of the project (WP4) has not yet been completed, part of the MEDIT dataset developed there has been used both to parameterize and validate the selected models. The vegetation dynamic model that have been used are:

1) the Joint UK Land Environment Simulator (JULES) (Clark et al. 2011), where three new Mediterranean Plant Functional Types (PFTs) have been defined and their key biochemical parameters adjusted based on our data

2) the TFS (Trait-based Forest Simulator, (Fyllas et al., in review), where algorithm developments have been made, in order for the model to be applicable at Mediterranean Forests.

The JULES model is a process-based model that simulates the fluxes of carbon, water, energy and momentum between the land and the atmosphere (Best et al. 2011, Clark et al. 2011). In the original version of the model, five PFTS were used to represent the dominant groups of plants around the globe. These PFTs are differentiated by their basic structural and functional characteristics. Vegetation dynamics are implemented as in the TRIFFID model. In later versions of JULES new PFTs have been added, to include new PFTs such as the broadleaved deciduous and evergreen. Here we use the MEDIT database to *a priori* define three new PFTs that could be included when simulating the dynamics of vegetation at areas surrounding the Mediterranean Basin. These PFTs are: the Mediterranean Evergreen Broadleaved (MEB) group, the Mediterranean Conifer (MC) group and the Mediterranean Deciduous Broadleaved (MDB) group, which are the focus of the MEDIT project. In this document we describe the implementation and validation of JULES at three Mediterranean Eddy Flux Tower sites, and evaluate to what extent it can be used along with the MEDIT dataset to accurately predict forest dynamics across the basin.

One of the current criticisms of large scale models such as JULES concerns their limited representation of functional plant diversity, as the relatively small number of PFTs used cannot express the wealth of potential responses to environmental shift and/or variability (Lavorel et al., 2007; Boulangeat et al., 2012; Fyllas et al., 2012). The Trait-based Forest Simulator (TFS) is a next-generation hybrid vegetation model that integrates small and large scale approaches (Fyllas et al., under review). It combines the standard algorithms of energy, water and carbon fluxes applied in large scale DGVMs with the individual level demographic processes that are the focus of smaller scale models. It can be used both at the stand and at the regional level to simulate the biochemical fluxes of various forest types. Importantly TFS can be implemented as either a classic DGVM (like JULES) applying PFT-specific parameters to the simulated vegetation or as traits-continuum model replacing the use of discrete functional traits values with the use of trait distributions to more realistically represent functional diversity in simulating vegetation dynamics. The TFS model was initially developed by the postdoctoral researcher for tropical forests and it was only working as a static/snapshot version (Fyllas et al., in review), i.e it required a predefined stand structure and simulations could only be made for a short time period. Within component C3 we developed the dynamic version of TFS, by adding a recruitment and a mortality algorithm. In addition data gathered from the MEDIT study sites were used to parameterise the model. In summary the developments made at TFS include: 1) application of a new photosynthesis scheme 2) development of the recruitment algorithm, 3) development of the mortality algorithm, 4) development/parameterisation of the stand initialisation algorithms, 5) development/parameterisation of the allometry algorithms, 6) parameterisation of the traits intercorrelations equations.

In this report the steps followed to link field-based MEDIT data with TFS are presented. The ability of TFS to simulate carbon and water fluxes at the point level and subsequently at a the ecosystem scale are presented in the accompanying Deliverable No 5 (D3.2).

Study Sites and Measured Functional Traits

A short description of the currently available MEDIT dataset will be presented here. The full description will be given when the corresponding component (WP4) will be completed. Within MEDIT we have already developed an extended dataset where tree-level functional characters and stand-level parameters have been measured for 49 plots at different Greek mountains. A map of the study sites that have already been censused is presented in Fig. 1. An altitudinal range between 374 to 1655 m above sea level (asl) has been achieved within the MEDIT dataset covering various forest types, and in particular the ones used for that are the focus of this project, i.e. the Mediterranean Evergreen Broadleaved (MEB), the Mediterranean Coniferous (MC), and the Mediterranean Deciduous Broadleaved (MDB) forests.

Figure 1: Map of study sites where individual level and stand level data have been gathered and analyzed.

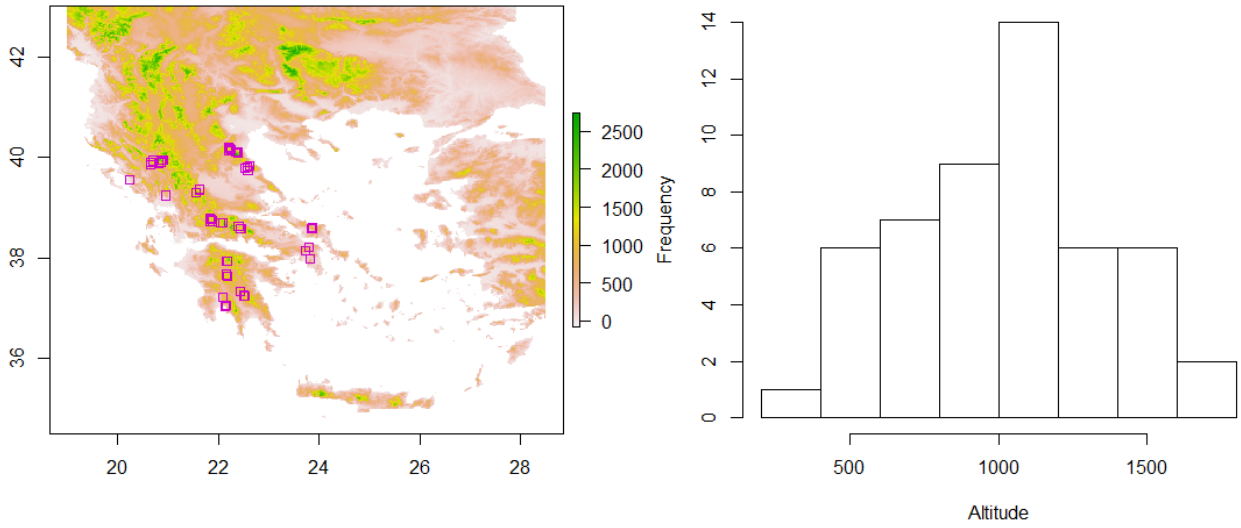

For most of the MEDIT study sites, a set of stand-level parameters including edaphic, biometric and climatic data are gathered. At the tree-level a set of biometric, dendrochronological and functional measurements are made. Currently the dataset includes 462 measurements of leaf and wood functional traits suites for 33 species as summarized in Table 1. In a subset of 295 individuals, leaf level CO_2 fluxes have also been quantified. We expect that our dataset will expand to around 700 trait measurements and 450 carbon flux measurements by the end of 2015. It should be noted that the species included in the dataset are considered the most dominant and common tree species found in the forest ecosystems covering the Greek peninsula. The leaf and wood trait measurements include estimation of leaf mass per area (M_A), leaf area (L_A), leaf thickness (L_T) as well as the leaf level concentrations of C, N, P, Ca, Mg, K and S, the wood density (WD) and in some cases the estimation of the leaf to sapwood area ratio (L_A/S_A). At a subset of the trees found in each plot around 15 light and CO_2 response curves are developed using a programmable script on the LICOR-6400 gas analyser, to estimate the carboxylation capacity (V_{max}), the maximum rate of electron transport (J_{max}), the maximum photosynthetic capacity (A_{max}) and the dark respiration of the leaf (R_{dark}). The biometric measurements made at the individual-level include the estimation of the diameter at breast height (dbh) and the height (H) of the tree. Along the 50 plots we have currently recorded more than 7700 individuals with around 4200 H=f(dbh) associations. At the plot-level apart of the total established biomass we also measure the LAI (leaf area index) of the plot at 15 points, the regeneration density at five 1x1 m^2 subplots, the soil depth, and a number of mechanical and chemical soil properties like pH, ECEC, the C, N, P, Ca, Mg, K concentrations as well as the mechanical properties and the water holding capacity of the first 30 cm. The climatic data are extracted from the WORLDCLIM dataset (Hijmans et al., 2005) and include 15 long-term climatological parameters. The way these data have been used to vegetation dynamics models is shortly described presented below.

Table 1: Summary table of studied species, their PFT classification, along with the number of individuals the functional traits of interest that have been measured for each one of them and used to paramerise the vegetation dynamics models

Species	PFT	Leaf and Wood Trait Measurements	Photosynthesis and Respiration
Abies borisii	MC	20	12
Abies cephalonica	MC	63	39
Acer campestre	MDB	6	3
Acer obtusatum	MDB	2	2
Acer platanoides	MDB	2	1
Arbutus andrachne	MEB	10	4
Arbutus unedo	MEB	10	2
Carpinus betulus	MDB	2	2
Carpinus orientalis	MDB	10	7
Castanea sativa	MDB	19	16
Cercis siliquastrum	MDB	2	2
Cistus creticus	Not used	5	
Cistus salviifolius	Not used	5	
Cornus mas	MDB	2	2
Corylus avellana	MDB	1	
Cotinus cogyria	MDB	5	3
Fagus sylvatica	MDB	47	37
Fraxinus excelsior	MDB	1	1
Fraxinus ornus	MDB	3	2
Ostrya carpinifolia	MDB	18	13
Phyllirea latifolia	MEB	12	5
Pinus halepensis	MC	19	3
Pinus nigra	MC	71	64
Pistacia terebinthus	MEB	5	1
Quercus cerris	MDB	19	11
Quercus coccifera	MEB	34	10
Quercus frainetto	MDB	40	34
Quercus ilex	MEB	9	4
Quercus pubescens	MDB	15	10
Quercus rotundifolia	MEB	2	2
Salix alba	MDB	1	1
Sorbus domestica	MDB	1	1
Tillia platyphyllos	MDB	1	1
		462	**295**

Development/parameterisation of DGVMs

JULES

Three new Mediterranean PFTs have been defined in JULES. A set of key parameters of the JULES model were selected and adjusted to better represent Mediterranean vegetation. These parameters include: the leaf dry mass per area (LMA), the nitrogen content expressed per mass and/or per area (Nmass, Narea), the carboxylation efficiency Vmax, the dark respiration rate, and the leaf turnover rate (g_{leaf}). These above parameters of the JULES model were changed to the ones extracted from the MEDIT database. The leaf turnover rate was estimated indirectly from the mean M_A per PFT and the equation $log_{10}(a) = 1.11 \cdot log_{10}(M_A) - 1.299$ (Osnas et al., 2013).

The following table and figures reports these changes.

Table 2: Parameters changed with the new Mediterranean PFTs. The first 3 columns are the standard JULES PFT values. The last 3 columns are extracted (mean values) from the MEDIT dataset.

PFTs	JULES Temperate Evergreen	JULES Temperate Deciduous	JULES Temperate Evergreen	MEDIT MEB	MEDIT MDB	MEDIT MC
LMA	140.3	82.3	226.3	132	62	196
Nmass	0.0144	0.021	0.0115	0.0123	0.0228	0.0109
Narea	2.02	1.73	2.6	1.62	1.41	2.14
Vmax	61.28	57.25	53.55	76.6	64.8	71.4
R_{dark}				2.15	1.13	1.67
g_{leaf}	0.50	0.50	0.50	0.95	0.41	1.47

In order to validate the predictive ability of the reparameterised JULES-DGVM we tested its performance at three eddy flux tower sites across the Mediterranean. Flux observations were obtained from the Fluxnet database (http://fluxnet.ornl.gov/). The variables of interest concern stand level carbon and water fluxes, in particular: Gross Primary Productivity (GPP), which is the total amount of carbon photosynthesised by vegetation, latent heat flux (LE), which expresses water fluxes and ecosystem respiration (Reco).

The test sites (Table 3) include:

- A evergreen deciduous shrubland in Italy, categorised as a MEB-PFT
- A conifer forest in Spain, categorised as a MC-PFT
- A deciduous broadleaved forest in Italy, categorised as a MDB-PFT.

Table 3: General Description of JULES Test sites

Site	Code	Lat	Lon	Vegetation	PFT used
El Saler	ES-ES1	39.3460	-0.3188	Coniferous Forest	MC
Castelporziano	IT-Cpz	41.7053	12.3761	Evergreen Broadleaved Forest	MEB
Roccarespampami1	IT-Ro1	42.4081	11.93	Deciduous Broadleaved Forest	MDB

Simulations over the period of interest for each one of the JULES validation sites are presented below. In the following graphs the observed values of GPP, LE and Reco are plotted along with the simulations following the original and re-parameterised PFTs. It should be noted that the model was forced to run with a predefined PFT set to the established vegetation at each one of the study sites.

JULES performed very poorly at the coniferous forest in Spain under both parameterizations. Both GPP and Reco were substantially underestimated. The latent heat fluxes did also not performed well and were out of phase in some time periods. This could be considered a bad model performance.

Figure 2: JULES simulations in a Mediterranean Coniferous Forest

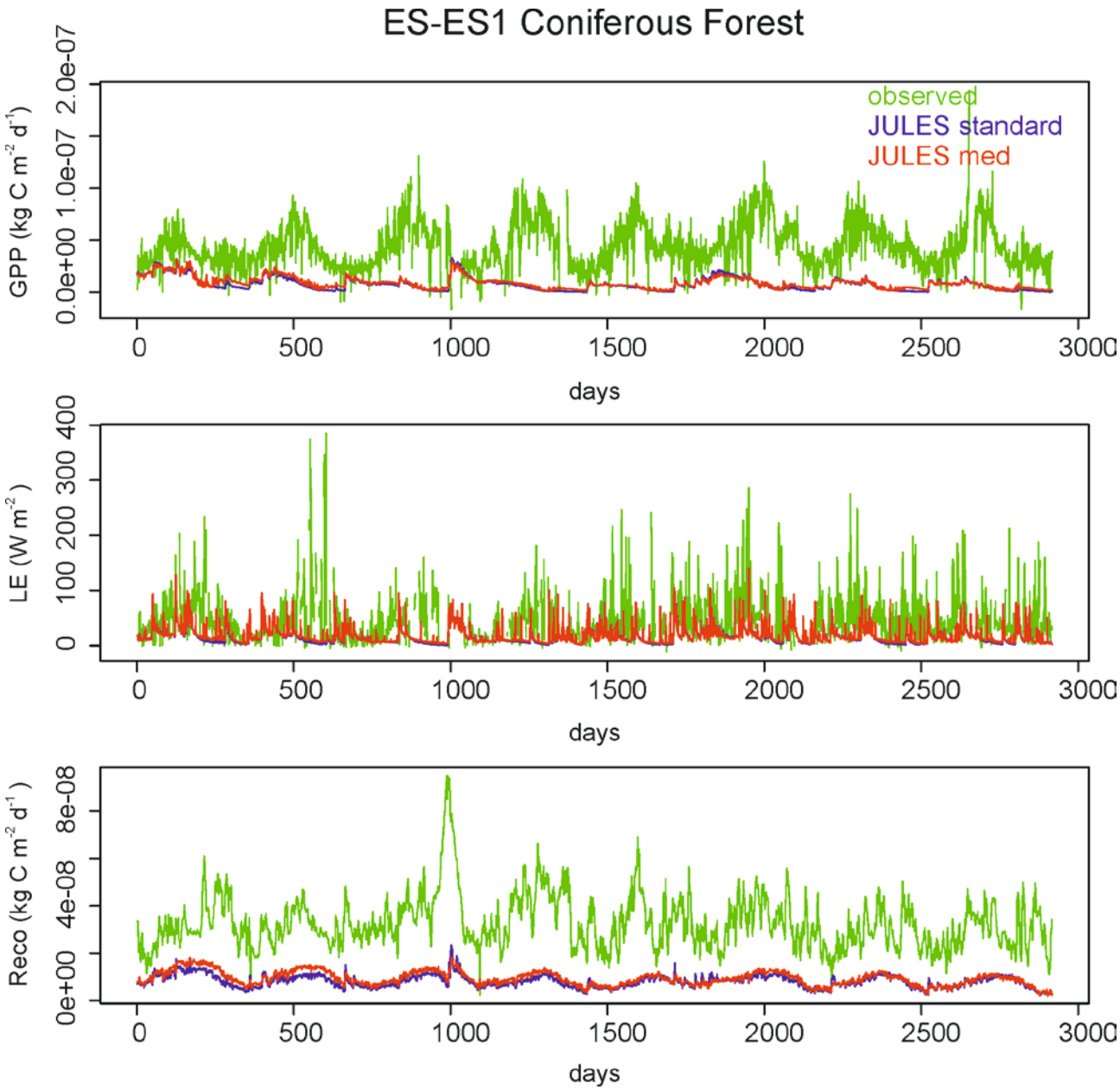

At the evergreen broadleaved forest in Italy simulations indicated a relatively better performance, but again it could not be considered adequate. Inclusion of Mediterranean PFTs did not substantially changed the performance of the model.

Figure 3: JULES simulations in a Mediterranean Evergreen Broadleaved Forest

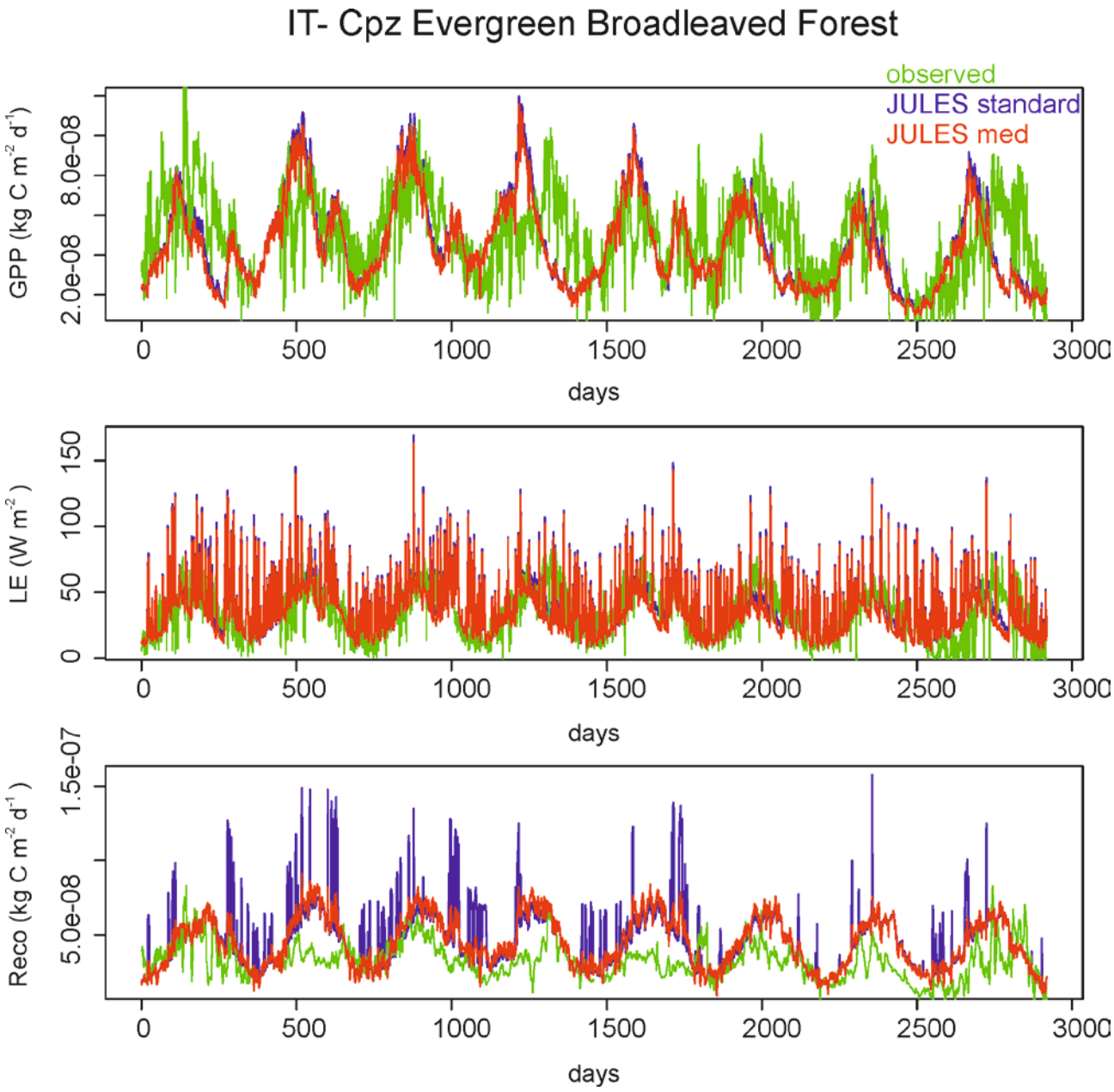

JULES performance at the deciduous broadleaved forest site in Italy is presented in the figure below. GPP and Reco were underestimated with a better performance for LE. Again inclusion of the Mediterranean PFTs did not substantially changed the performance of the model.

Figure 4: JULES simulations in a Mediterranean Deciduous Broadleaved Forest

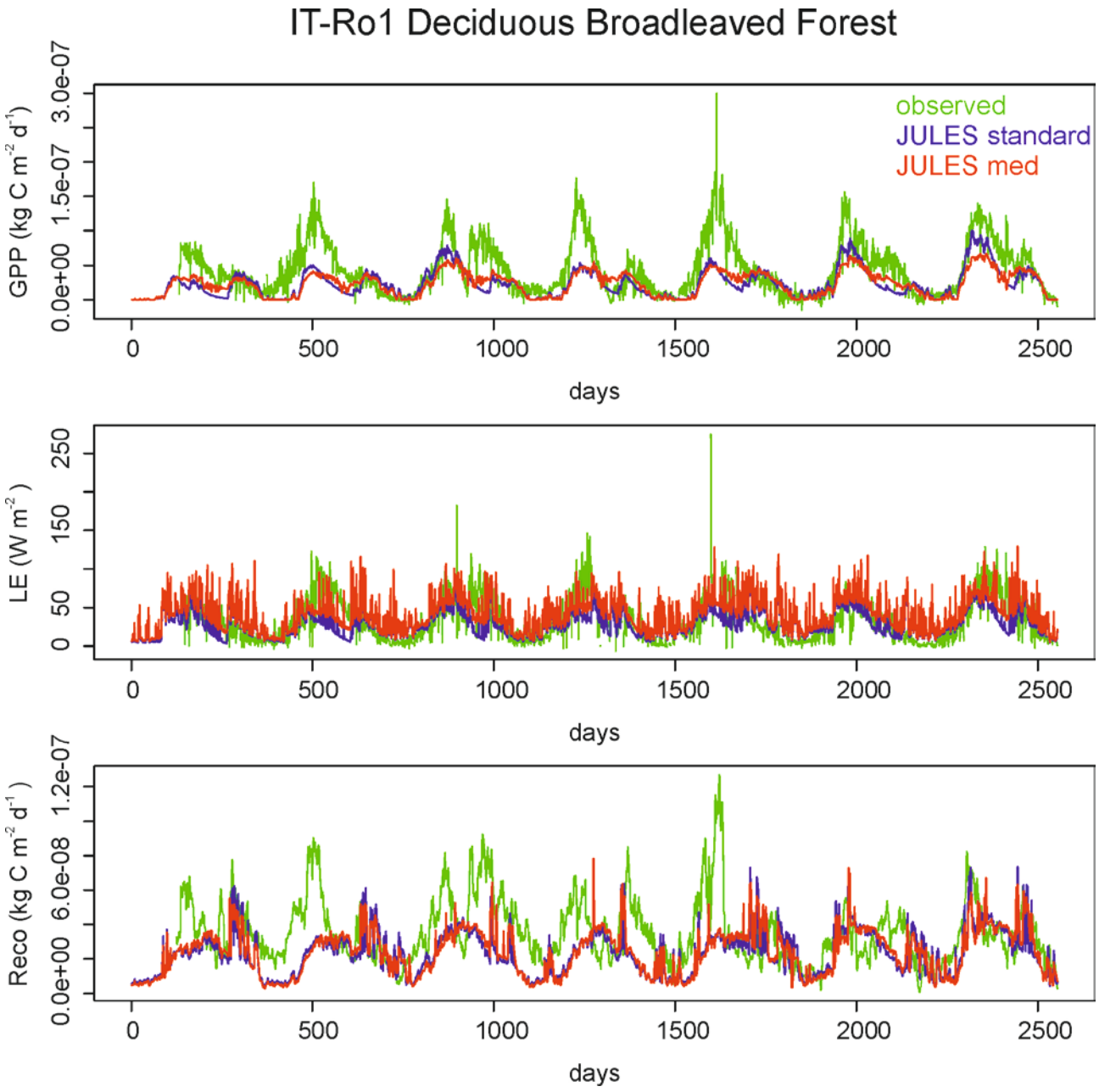

Conclusions

At the three Mediterranean forest sites that the model has been evaluated, it has not shown a promising performance. Furthermore, and probably more importantly the parameters that can be extracted from the MEDIT dataset developed in C4 do not seem to substantially change the model behavior. A simulation exercise along the Mediterranean Basin with JULES is presented in the accompanying deliverable D3.2.

TFS

TFS is an individual-based model that uses functional traits data to represent different plant strategies for resource acquisition and allocation (Fyllas et al., in review). In TFS the use of PFTs is replaced by traits distribution and thus a continuum of plant strategies rather than discrete types is implemented. The four key functional characters are leaf dry mass per area (LMA), leaf N and P concentration (N_L, P_L) and wood density (*WD*). In the following paragraphs most allometric, functional and biochemical equations will be expressed on the basis of these four characters and the data gathered under the MEDIT field campaign protocol. The new algorithms that have been developed are: 1) a new photosynthesis scheme 2) a recruitment algorithm, 3) a mortality algorithm, 4) a parameterisation of the stand initialisation algorithm, 5) a new tree allometry algorithm as well as 6) parameterisation of various traits intercorrelations equations. The new version of the TFS model is available from request from the author.

Development of a new Photosynthesis Scheme

The static (older) version of the TFS model uses a detailed (hourly) photosynthetic algorithm that couples the Farquhar et al. (1980) model with the Medlyn et al. (2011) stomatal conductance equation. This representation of photosynthesis is computationally expensive when solved for each one of the tree that are simulated in the stand. Thus a simplified daily photosynthesis scheme (Chen et al. 1999) based on the same principles has been coded into the TFS. This algorithm is described elsewhere and will not be detailed here. In the appendix of this document the JAVA code is also given. We will just refer to the changes made in order to be applied for Mediterranean forest species:

- Vmax and Jmax are estimated based on the empirical equations from Walker et al. (2014), where: $V_{\max} = f(LMA, N), J_{\max} = f(V_{\max})$
- Temperature sensitivities are given estimated from Bernachi et al. (2004).
- Lead dark respiration is estimated as a proportion of Vmax

Development of the Recruitment Algorithm

A new recruitment algorithm that is needed to have a dynamic version of TFS was developed. The purpose of this submodel is to estimate a bioticaly controlled regeneration density and to inherit the appropriate functional traits to the recruits. Light was assumed to be the most important component of recruitment limitation LAI was used as the variable controlling light availability at the forest floor. Based on the range of recruitment densities observed in the MEDIT field campaign two functional equations (a linear and an exponential decrease) were developed. A validation exercise of these two models indicated a similar performance (Fig. 5). However the exponential one was preferred as it also provides the assumption of seeds income from adjacent plots.

Figure 5: The two alternative recruitment limitation models. The linear one illustrated with a red colour and the exponential one with a blue. A similar performance of TFS was observed.

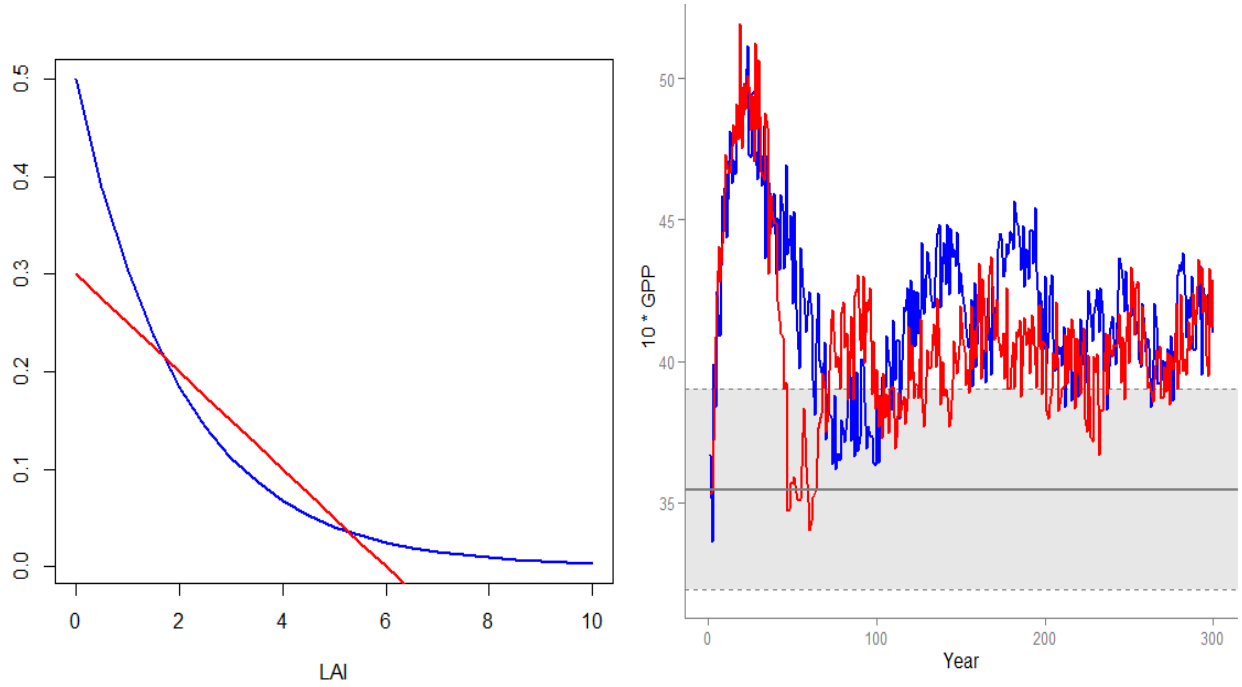

The traits inheritance method is considered to be a crucial one as it specifies the trait distribution of the next generations and thus the future dynamics of the simulated forests. The assumptions made to build this model were:

- At each time step only mature trees are considered to contribute to the regeneration/genetic pool and thus have the potential to pass their genes and in our case their traits values to saplings. As mature we consider trees with a diameter (D) greater than 10 cm.
- Saplings are inheriting their traits from the distribution available in the regeneration pool. The values of traits don't have to be exactly the same with the ones in this pool, but they have to follow its distributional properties. This assumption enables trait plasticity.
- Saplings have to survive for ten years before becoming mature trees and contribute to the stand biomass and genetic pool.

Development of the Mortality Algorithm

The mortality component of the model based on the equation suggested in Martinez Vilalta et al. (2010). This equation was developed for tree species found in Spain under a similar range of climatic conditions. It uses wood density (WD) as the sole predictor to estimate an annual background mortality rate:

$$\Pi_R = 0.51e^{(-3.56 \cdot WD)}$$

Tree Architecture

Here we use the tree height -dbh data to parameterize the allometry used in TFS. The overall, species independent H=f(dbh) relationship can be expressed with an exponential equation as shown in Fig. 6. The coefficient estimates of the equation ($H = e^{\alpha+\beta\cdot\log(dbh)}$) with the overall model yielding an R^2 = 0.84, are:

	estimate	st error	p
α	0.580	0.008	<0.001
β	0.605	0.004	<0.001

Figure 6: Species independent H-dbh equation

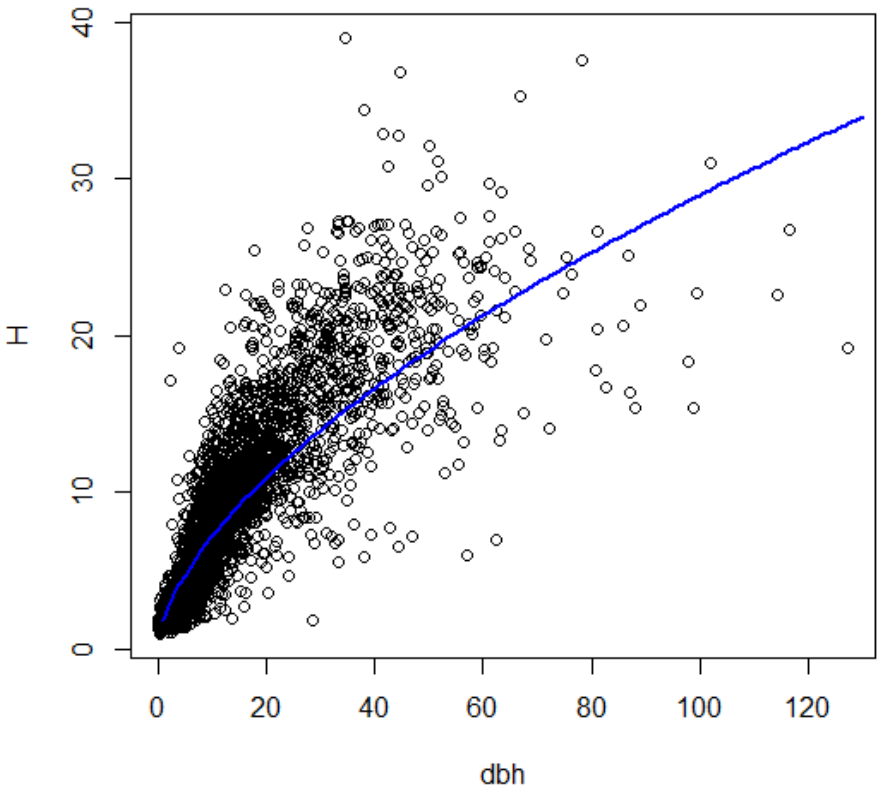

An alternative formulation of the H-dbh relationship, that takes into account the shade tolerance of a species as well as its wood strength, as described in Deitze et al. (2008), was also used in this version of the model. Here the height allometric equation is expressed as:

$$H = e^{\alpha+\beta\cdot ST+\gamma\cdot WS\ +(\delta+\varepsilon\cdot ST+\zeta\cdot WS)\cdot log\,(dbh)}$$

with α=0.32 , β=0.03, γ=-0.02, δ=0.59, ε=0.0, ζ=0.01. Here *ST* expresses the shade tolerance of a species/individual and we assume that it can be approximated from its M_A, with higher M_A indicating a higher shade tolerance. Five shade tolerance classes were defined as in Deitze et al. (2008) with increasing *ST* indicating lower shade tolerance. *WS* expresses the wood mechanical strength and we assumed that it can approximated by the value of the *WD* of each species/individual. A normalized measure of *WS* was calculated as: $WS = \frac{WD-\widehat{WD}}{sd\,(WD)}$ with WD the

value of each species/individual, $\widehat{WD}$ the mean value of the community it belongs and *sd(WD)* the standard deviation of *WD* for this community. These new equations were used in TFS along with the crown area (C_A) and crown depth (C_D) presented in Deitze et al. 2008 to redefine the allometry for Temperate and Mediterranean forests. Figure 7 (a&b) summarizes the new allometric scheme in TFS. In general shade intolerant trees are higher for a given diameter while shade tolerant trees have a greater leaf biomass. Trees with greater wood mechanical strength have a greater leaf biomass as well.

Figure 7a: Trait-based tree allometry, accounting for shade tolerance

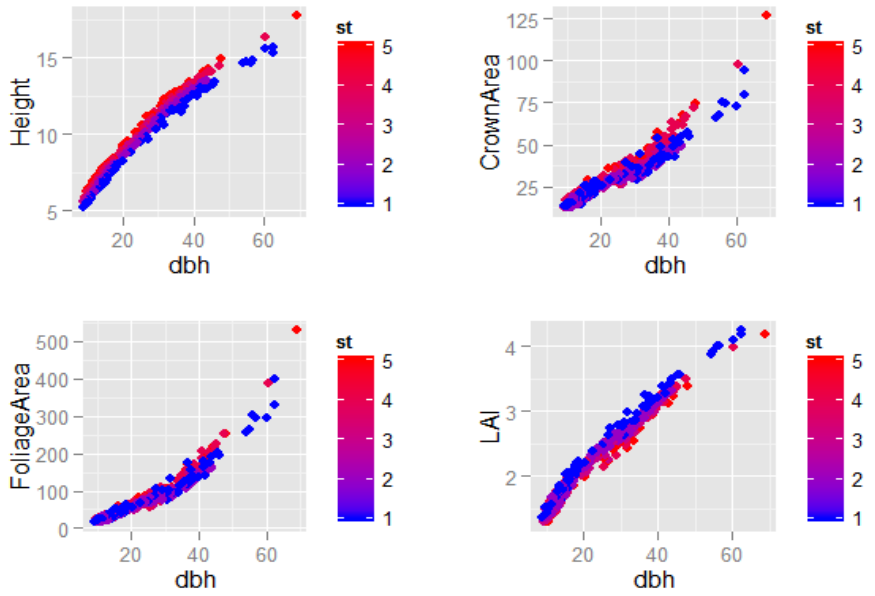

Figure 7b: Trait-based tree allometry, accounting for shade tolerance

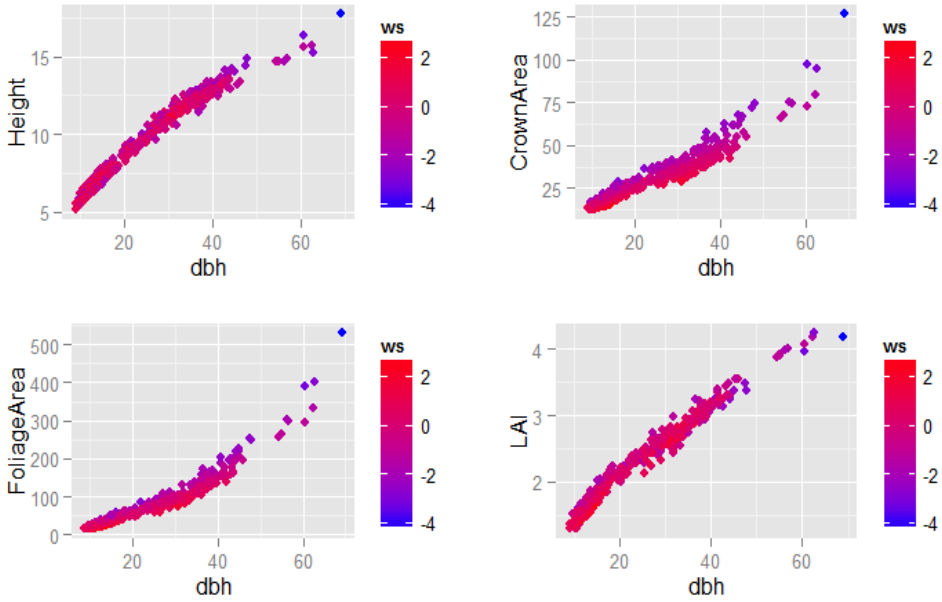

Stand Structure - Size Class Distribution

The tree-by-tree diameter data (Fig. 7) gathered in the 35 of the MEDIT plots were used here to develop a stand structure generation algorithm. Thus apart from initializing the model with the plot-specific data we were interested to develop an algorithm to randomly (but based on observation) deploy a stand structure based on classic resampling techniques. To achieve this, we fitted a set of distribution to the tree-by-tree diameter at breast height (dbh) data and explored which of those distributions better explained the size-class structure of the stand. The evaluated distributions were: the Weibull, the Gamma, the Normal and the Log-normal. A summary table of the fitting parameters for each distribution at each plot is presented in Table 2.

The fit of the distributions was tested by considering the Akaike Information Criterion (AIC), with the minimum value indicating the best model. As illustrated in Table 2 in most plots the *Log-normal* and the *Weibull* distributions described better the structure of the stand. Thus a stand structure generation algorithm based on the *Log-normal* distribution was created and built in TFS.

Figure 8: Distribution of dbh in the 36 MEDIT plots as described by the *Log-normal* distribution. Different line colours indicate different plot and the thick black line indicated the overall distribution.

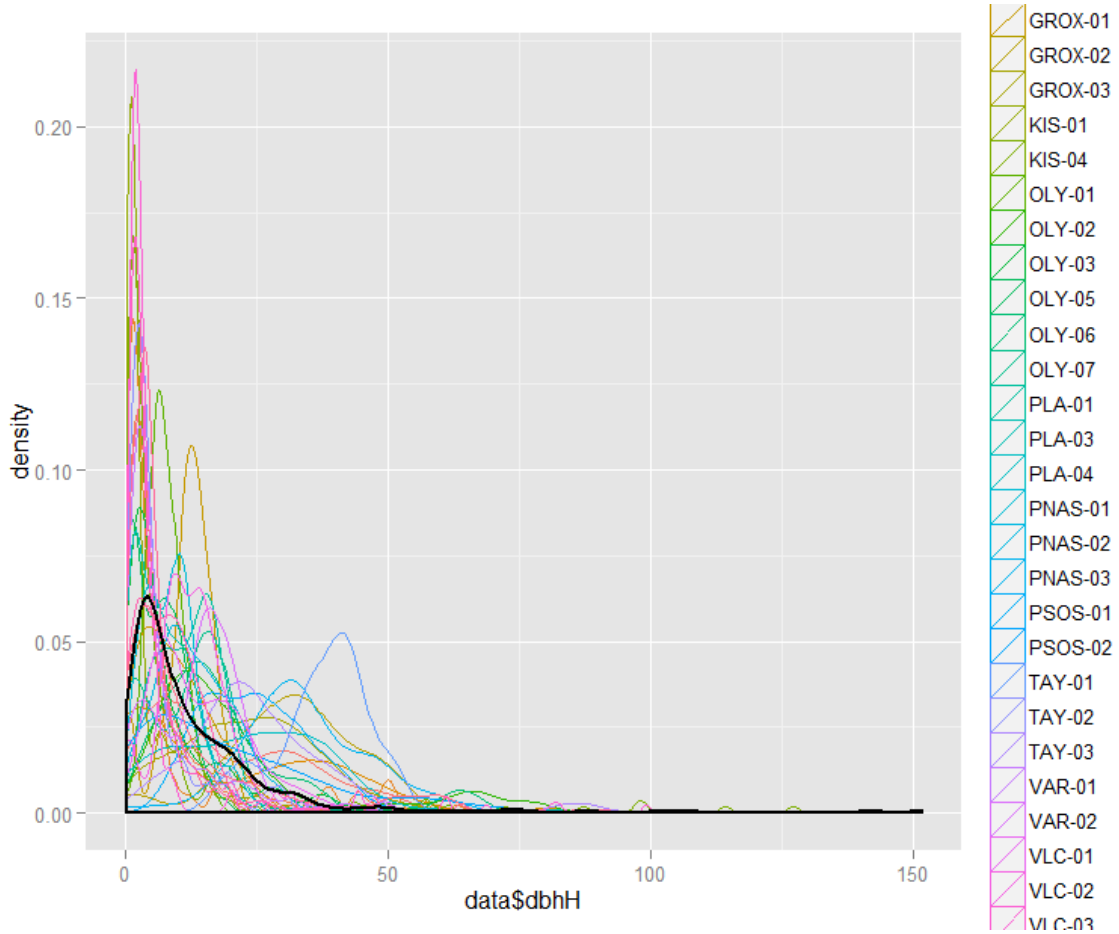

Table 4: Summary table of the potential distributions describing the stand structure at typical Mediterranean and mountainous Mediterranean forests. The minimum AIC value is highlighted with bold values, indicating the distribution better describing the data.

	Weibull			Gamma			Normal			LogNormal		
Plot	**shape**	**scale**	**AIC**	**shape**	**rate**	**AIC**	**mean**	**sd**	**AIC**	**mean**	**sd**	**AIC**
DOX-01	0.68	7.31	789	0.58	0.06	802	10.12	16.32	1057	1.24	1.42	**757**
DOX-02	0.85	17.08	612	0.78	0.04	612	18.54	18.20	678	2.16	1.39	**612**
DOX-03	1.11	12.56	1222	1.29	0.11	**1218**	12.04	12.30	1379	2.05	1.00	1219
DIR-01	1.33	20.54	**540**	1.56	0.08	540	18.87	14.07	565	2.58	0.92	545
DIR-02	0.92	7.13	1265	0.97	0.13	1267	7.45	9.42	1542	1.41	1.09	**1229**
TAY-01	3.15	44.24	353	10.90	0.27	345	39.84	12.50	351	3.64	0.31	**345**
TAY-02	0.96	6.42	1184	1.04	0.16	1184	6.54	7.75	1425	1.32	1.06	**1154**
TAY-03	1.83	29.53	229	3.29	0.13	227	26.18	15.15	236	3.11	0.60	**229**
PNAS-01	1.57	11.03	**1583**	2.08	0.21	1586	9.89	6.43	1644	2.03	0.80	1616
PNAS-02	1.70	14.97	**2150**	2.27	0.17	2165	13.41	7.96	2198	2.36	0.80	2239
PNAS-03	2.19	41.54	**555**	3.85	0.10	558	37.02	17.15	558	3.48	0.65	584
PSOS-01	2.79	27.66	**728**	6.20	0.25	727	24.57	9.58	732	3.12	0.42	731
PSOS-02	1.11	22.44	**759**	1.22	0.06	759	21.53	19.50	820	2.61	1.04	760
VAR-01	0.90	8.21	1967	0.91	0.10	1973	8.74	11.19	2389	1.53	1.14	**1918**
VAR-02	1.61	14.92	888	1.71	0.13	902	13.57	7.72	**884**	2.29	1.01	949
GROX-01	2.53	13.28	1732	2.79	0.23	1827	12.07	4.70	**1660**	2.30	0.85	1987
GROX-02	2.08	35.78	381	2.40	0.07	392	32.50	14.39	**372**	3.26	0.99	424
GROX-03	1.64	28.61	**659**	2.04	0.08	664	25.77	15.57	670	2.98	0.90	691
PLA-01	1.82	15.85	**1188**	2.72	0.19	1191	14.09	8.04	1216	2.45	0.70	1217
PLA-03	1.15	8.59	**2208**	1.20	0.15	2211	8.18	6.73	2378	1.63	1.15	2282
PLA-04	1.55	26.51	**678**	1.82	0.08	683	24.00	15.00	689	2.88	0.92	703
ZAG-01	1.06	10.65	1426	1.16	0.11	**1425**	10.40	11.14	1635	1.85	1.08	1431
ZAG-02	0.90	6.78	2211	0.97	0.13	2220	7.24	11.63	2885	1.38	1.05	**2123**
ZAG-03	0.84	13.40	1457	0.82	0.05	1463	14.87	19.77	1748	1.97	1.24	**1433**
VLC-01	1.60	16.71	**1100**	2.20	0.15	1101	14.96	9.68	1140	2.46	0.78	1124
VLC-02	1.53	14.57	**2043**	1.75	0.13	2066	13.29	8.34	2085	2.27	1.06	2210
VLC-03	0.70	6.38	1228	0.62	0.07	1264	8.95	20.06	1798	1.21	1.16	**1131**
VLC-04	0.94	5.68	1686	1.00	0.17	1688	5.87	7.24	2071	1.19	1.08	**1635**
OLY-01	1.34	11.75	2368	2.08	0.19	2331	10.67	9.54	2642	2.11	0.72	**2305**
OLY-02	1.22	26.66	514	1.51	0.06	512	24.83	21.65	552	2.85	0.89	**510**
OLY-03	0.92	9.38	2002	0.94	0.10	2006	9.80	11.74	2372	1.67	1.14	**1968**
OLY-05	0.94	6.76	**1849**	0.94	0.13	1850	6.97	8.23	2219	1.32	1.24	1859
OLY-06	1.43	22.72	680	1.98	0.10	676	20.52	15.49	719	2.75	0.77	**676**
OLY-07	0.89	12.40	**824**	0.90	0.07	827	13.20	24.06	1062	1.93	1.27	829
KIS-01	0.69	3.96	2469	0.60	0.11	2512	5.31	8.81	3526	0.63	1.46	**2383**
KIS-04	0.67	6.34	1060	0.58	0.06	1092	9.33	22.05	1583	1.16	1.30	**997**

Leaf Structure and Chemistry

The foliage data gathered for more than 460 individual trees in the 50 MEDIT plots were analyzed using common statistical techniques like correlation tests and standardized major axis regression. Our aim here was to identify relationships between functional traits that are general enough to be used across species and sites. The leaf functional traits of interest were leaf thickness (L_T), leaf dry matter content (L_{DMC}), leaf dry mass per area (M_A), and the per cent concentration of C, N, P. These functional characters are known to be linked within the "worldwide leaf economic spectrum" (Reich et al., 1997; Wright et al., 2004), that expresses a coordinated variation along resource gradients spanning from a low return strategy (high M_A and C, low N and P) to a high return strategy (low M_A and C, high N and P). Dynamic vegetation models often use these relationships to represent discrete plant strategies. Although an axis of common variation exists for those characters, trait-shifts along climate zones are of sufficient magnitude and have major implications for plant dry mass and nutrient economics (Wright et al., 2005). In Table 5 and Fig. 8 we summarize the most important associations identified and implemented in the TFS modelling framework. These equations are used within TFS to parameterize the foliage retention time, the photosynthesis and respiration models and the mortality algorithm and thus introduce a general "fast-slow plant economic spectrum" (Reich, 2014).

Table 5: Pearson's r and associated significance along with the coefficient estimates of the SMA regression for the relationships between key leaf structural and chemical traits. SMA was fitted to the log10 transformed data thus the back-transformed equation is: Y=10^(a+b(log$_{10}$(X))

Y	X	r	p	a	b	N
L_T (mm)	M_A (g m^{-2})	0.83	0.00	-3.01	1.22	463
L_{DMC} (g g^{-1})	M_A (g m^{-2})	0.45	0.00	-1.17	0.39	465
N(%)	M_A (g m^{-2})	-0.82	0.00	1.47	-0.63	463
P(%)	M_A (g m^{-2})	-0.66	0.00	0.39	-0.68	454

Figure 9: Standardized Major Axis regression lines for the leaf structural and chemical traits of interest.

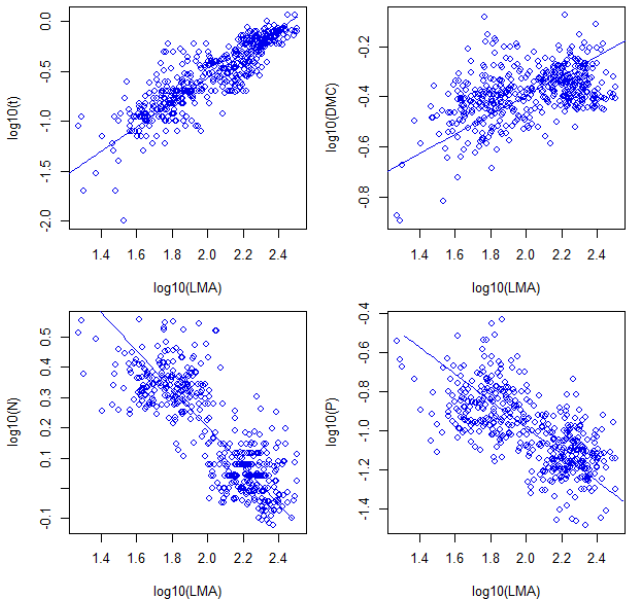

Leaf Carbon Fluxes

The data gathered using the LICOR-6400 infrared leaf gas analyzer were used to develop photosynthetic curves along CO_2 (A-Ci) and light (A-I) availability gradients. Up to now, around 30 key forest tree species found in Greece have been measured at least at one site and their light (A_{sat}) and light & CO_2 (A_{max}) saturated photosynthetic rate have been calculated, along with the maximum carboxylation (V_{max}) and electron transport rate (J_{max}). For the same species the leaf dark respiration (R_{dark}) has also been calculated. These measurements have been made to almost 300 individual trees in order to quantify the spatial variation of those parameters. All these measurements are required to parameterize the carbon flux algorithm of the TFS model while they can also serve as a basis for parameterising the PFT level variables of JULES.

We used multiple linear regressions to find the best predictive model of V_{max}, J_{max}, A_{sat} and R_{dark} using structural and chemical leaf traits as predictive variables. The table below summarizes optimum parameterization that can be used for the trait-based vegetation dynamics model.

Table 6: Predictive multiple linear regressions of key traits related to leaf carbon fluxes. Bold values indicate statistically significant estimates and the predictive ability of the regression is indicated by its R^2.

	intercept	LMA(g m^{-2})	N(%)	P(%)	R^2
V_{max} (μmol m^{-2} s^{-1})	**1.23**	**0.21**	**0.24**	-0.11	0.051
J_{max} (μmol m^{-2} s^{-1})	**1.12**	**0.20**	0.18	**-0.32**	0.178
A_{sat} (μmol m^{-2} s^{-1})	**0.35**	**0.21**	**0.69**	-0.09	0.146
R_{dark} (μmol m^{-2} s^{-1})	**-0.90**	**0.53**	**0.26**	0.13	0.265

Conclusions

In the accompanying report (MEDIT Report No 5: "Report on Vegetation Dynamics across the Mediterranean basin", validation exercises for TFS are presented. This hybrid model presents a better behaviour and more importantly it can be strongly linked with the MEDIT dataset. So we will concentrate our efforts on further developing the TFS model and not JULES.

Acknowledgments

The research project is implemented within the framework of the Action «Supporting Postdoctoral Researchers» of the Operational Program «Education and Lifelong Learning» (Action's beneficiary: General Secretariat for Research and Technology), and is co-financed by the European Social Fund (ESF) and the Greek State.

This work used eddy covariance data acquired by the FLUXNET community and in particular by the following networks: AmeriFlux (U.S.Department of Energy, Biological and Environmental Research, Terrestrial Carbon Program (DE-FG02 04ER63917 and DE-FG02 - 04ER63911)), AfriFlux, AsiaFlux, CarboAfrica, CarboEuropeIP, CarboItaly, CarboMont, ChinaFlux, Fluxnet-Canada, (supported by CFCAS, NSERC, BIOCAP, Environment Canada, and NRCan), GreenGrass, KoFlux, LBA, NECC, OzFlux, TCOS-Siberia, USCCC. We acknowledge the financial support to the eddy covariance data harmonization provided by CarboEuropeIP, FAO-GTOS-TCO, iLEAPS ,Max Planck Institute for Biogeochemistry, National Science Foundation, University of Tuscia, Université Laval and

Environment Canada and US Department of Energy and the database development and technical support from Berkeley Water Center, Lawrence Berkeley National Laboratory, Microsoft Research eScience, Oak Ridge National Laboratory, University of California - Berkeley, University of Virginia.

Appendix

Java Code for the Chen et al 1999 photosynthesis scheme as implemented in TFS.

```
case 2: // Chen 1999, Liu 1999 2002, Schwalm 2004

//// Global Vmax, Jmax = f(SLA,N,P)  Walker et al. 2014
        VLmax25 = Math.exp( 1.993+2.555*Math.log(NLa)- 0.372*Math.log(1.0/LMA) +
          0.422*Math.log(NLa)*Math.log(1.0/LMA)  );
        TempLK  = aday.Tm + 273.15;
        VLmax   = VLmax25*Math.exp(26.35 -(65330.0/(Rgas*TempLK)));
        Vm      = this.VLmax;
        Jmax25  = Math.exp(1.197+0.847*Math.log(VLmax25));
        Jmax    = Math.exp(1.197+0.847*Math.log(VLmax));

//////  Temperature Sensitivities based on  Bernacchi 2004
        Kc    =  Math.exp(38.05 - 79430.0/(Rgas*TempLK))*Math.pow(10, -6)*aday.Press_pa;
        Ko    =  Math.exp(20.30 - 36380.0/(Rgas*TempLK))*Math.pow(10, -3)*aday.Press_pa;
        K     =  Kc*(1.0+O2/Ko);
        Gamma  =  Math.exp(19.02 -37830.0/(Rgas*TempLK))*Math.pow(10, -6)*aday.Press_pa
        Ca    =  CO2_ppm*Math.pow(10,-6)*aday.Press_pa;


////    Dark Respiration
        double Rd25=0.015*VLmax25;
        Rd = Rd25*Math.exp(18.72 -(46390.0/(Rgas*TempLK)));

        double omega = 0.5; //foliage clumping
        double C     = 0.07*omega*aday.Sbeam*(1.1-0.1*LAI)*Math.exp(-1.0*aday.sin_bet);
        Qunder       = aday.Sdiff*Math.exp(-0.55*omega*LAI/(0.537+0.025*LAI));
        Qshade       = (aday.Sdiff-Qunder)/LAI+C;
        Qsun         = aday.Sbeam*Math.cos(Math.toRadians(60.0))/aday.sin_bet+Qshade;

        PPFDnoon_shade = (1.0/aday.Length)*2.3*Math.pow(10,6)*Qshade; // 2.3 , 2.0 works
        PPFDnoon_sun   = (1.0/aday.Length)*2.3*Math.pow(10,6)*Qsun;   // 2.3 , 2.0 works

        PPFDnoon_sun   = PPFDnoon_sun/LAI;
        PPFDnoon_shade = PPFDnoon_shade/LAI;


        if (this.inCanopyLayer <=1){   // canopy tree - equivalent to sun leaf

        // f_ppfd
           f_ppfd= (PPFDnoon_sun*PPFDcoef)/(1.0+PPFDnoon_sun*PPFDcoef);
           f_ppfd= Math.max(f_ppfd,0.000001);

        // f_T
           if (aday.Tm<=Topt) { f_T=Math.log(aday.Tm)/Math.log(Topt);}
           else            { f_T=Math.cos( (pi/2.0)*(aday.Tm-Topt)/(Trange-Topt) ); }
           if (aday.Tm<1.0)   { f_T=0.000001;}
           f_T=Math.min(f_T, 1.0);f_T=Math.max(f_T, 0.0);
```

```
        // f_Tmin
           if (aday.Tmin>0.0)   { f_Tmin=1.0;}
           if (aday.Tmin<=0.0)  { f_Tmin=1.0+0.0125*aday.Tmin;}
           if (aday.Tmin<Tcrit) { f_Tmin=0.000001;}


        // f_vpd
           double vpd=aday.VPDa;
           if   (vpd<VPDopen)   { f_vpd=1.0;}
           else {f_vpd=(VPDclose-vpd)/(VPDclose-VPDopen);}
           if   (vpd>=VPDclose) { f_vpd=0.000001;}

        // f_swp
           if (SWP>=SWPopen)  { f_swp=1.0; }
           else {f_swp= (SWPclose-SWP)/(SWPclose-SWPopen); }
           if (SWP<=SWPclose) { f_swp=0.000001; }


           f_all = Math.min(f_ppfd,f_T);
           f_all = Math.min(f_all,f_Tmin);
           f_all = Math.min(f_all,f_vpd);
           f_all = Math.min(f_all,f_swp);


// Stomatal Conductance
           gs    = gs_max*f_all;
           gnoon = gs*Math.pow(10,6)/(1.6*Rgas*(aday.Tm+273.15));


           aAc=Math.pow(K+Ca,2.0);
           bAc=2.0*(2.0*Gamma+K-Ca)*Vm+2.0*(Ca+K)*Rd;
           cAc=Math.pow(Vm-Rd,2.0);
           dAc=Math.sqrt(aAc*gnoon*gnoon+bAc*gnoon+cAc);


           Ac=(0.635/gnoon)*( Math.sqrt(aAc)*Math.pow(gnoon,2.0)/2.0
             + Math.sqrt(cAc)*gnoon  - ((2.0*aAc*gnoon+bAc)/(4.0*aAc))*dAc
             + bAc*Math.sqrt(cAc)/(4.0*aAc)
             + (Math.pow(bAc,2.0)- 4.0*aAc*cAc)/(8.0*Math.pow(aAc,1.5))
             * Math.log( (2.0*aAc*gnoon+bAc+2.0*Math.sqrt(aAc)*dAc)/(bAc+2.0*Math.sqrt(aAc)*Math.sqrt(cAc)) ) );


           J= Jmax*PPFDnoon_sun/(PPFDnoon_sun+2.1*Jmax);

           aAj= Math.pow(2.3*Gamma+Ca,2.0);
           bAj= 0.4*(4.3*Gamma-Ca)*J+2.0*(Ca+2.3*Gamma)*Rd;
           cAj= Math.pow(0.2*J-Rd,2);
           dAj= Math.sqrt(aAj*gnoon*gnoon+bAj*gnoon+cAj);


           Aj=(0.635/gnoon)*( Math.sqrt(aAj)*Math.pow(gnoon,2.0)/2.0
             + Math.sqrt(cAj)*gnoon  - ((2.0*aAj*gnoon+bAj)/(4.0*aAj))*dAj
             + bAj*Math.sqrt(cAj)/(4.0*aAj)
             + (Math.pow(bAj,2.0)- 4.0*aAj*cAj)/(8.0*Math.pow(aAj,1.5))
             * Math.log( (2.0*aAj*gnoon+bAj+2.0*Math.sqrt(aAj)*dAj)  /(bAj+2.0*Math.sqrt(aAj)*Math.sqrt(cAj)) ) );

           this.Ax=Math.min(Ac, Ac);
```

```
            Aday=Math.pow(10, -6)*(aday.Length)*Ax*LAI;  // [mol C m-2 d-1]

            rv= Math.pow(gbl*(gs+gcu)/(gbl+gs+gcu),-1.0);


            double air_dens =  1.204;            //(kg m-3)
            double cp = 1013.0;                 //(J kg-1 C-1)
            double sboltz = 5.6697*Math.pow(10,-8);//(W m-2 C-4)
            double l_vap= 2.45*Math.pow(10,6);     //(J kg-1) latent heat vaporation of water

            rr = air_dens*cp/(4.0*sboltz*Math.pow(aday.Tm+273.15,3));
            rc = rh*rr/(rh+rr);

            double SF=2.0; // shape factor converts from projected to total SLA;
            ET_day_mm =
((Math.pow(10,6)*aday.Sod/aday.Length)+air_dens*cp*aday.VPDa/rc)/(aday.Press_pa*cp*rv/(0.6219*l_vap*rc +
1000.0*aday.sigma) )*(aday.Length*SF*LAI/l_vap);
        }


        else{ // sub - canopy tree  equivalent to shade leaf

        // f_ppfd
//              PPFDnoon_shade = 2.3*Math.pow(10,6)*aday.Sdiff/aday.Length;
            f_ppfd= (PPFDnoon_shade*PPFDcoef)/(1.0+PPFDnoon_shade*PPFDcoef);
            f_ppfd= Math.max(f_ppfd,0.00001);

        // f_T
            if (aday.Tm<=Topt) { f_T=Math.log(aday.Tm)/Math.log(Topt);}
            else             { f_T=Math.cos( (pi/2.0)*(aday.Tm-Topt)/(Trange-Topt) ); }
            if (aday.Tm<1.0)   { f_T=0.00001;}

        // f_Tmin
            if (aday.Tmin>0.0)   { f_Tmin=1.0;}
            if (aday.Tmin<=0.0)  { f_Tmin=1.0+0.0125*aday.Tmin;}
            if (aday.Tmin<Tcrit) { f_Tmin=0.00001;}


        // f_vpd
            double vpd=aday.VPDa;
            if (vpd<VPDopen)   { f_vpd=1.0;}
            if (vpd<VPDclose)  { f_vpd=(VPDclose-vpd)/(VPDclose-VPDopen);}
            if (vpd>=VPDclose) { f_vpd=0.00001;}


        // f_swp
            if (SWP>=SWPopen)  { f_swp=1.0; }
            else {f_swp= (SWPclose-SWP)/(SWPclose-SWPopen); }
            if (SWP<=SWPclose) { f_swp=0.00001; }

            f_all = Math.min(f_ppfd,f_T);
            f_all = Math.min(f_all,f_Tmin);
            f_all = Math.min(f_all,f_vpd);
            f_all = Math.min(f_all,f_swp);

//              f_all=Math.pow(f_ppfd*f_T*f_Tmin*f_vpd*f_swp,1.0/5.0);

// Stomatal Conductance
            gs    = gs_max*f_all;//
```

```
            gnoon = gs*Math.pow(10,6)/(1.6*Rgas*(aday.Tm+273.15));


            aAc=Math.pow(K+Ca,2.0);
            bAc=2.0*(2.0*Gamma+K-Ca)*Vm+2.0*(Ca+K)*Rd;
            cAc=Math.pow(Vm-Rd,2.0);
            dAc=Math.sqrt(aAc*gnoon*gnoon+bAc*gnoon+cAc);


            Ac=(0.635/gnoon)*( Math.sqrt(aAc)*Math.pow(gnoon,2.0)/2.0
              + Math.sqrt(cAc)*gnoon  - ((2.0*aAc*gnoon+bAc)/(4.0*aAc))*dAc
              + bAc*Math.sqrt(cAc)/(4.0*aAc)
              + (Math.pow(bAc,2.0)- 4.0*aAc*cAc)/(8.0*Math.pow(aAc,1.5))
              * Math.log( (2.0*aAc*gnoon+bAc+2.0*Math.sqrt(aAc)*dAc)/(bAc+2.0*Math.sqrt(aAc)*Math.sqrt(cAc)) ) );

            J= Jmax*PPFDnoon_shade/(PPFDnoon_sun+2.1*Jmax);

            aAj= Math.pow(2.3*Gamma+Ca,2.0);
            bAj= 0.4*(4.3*Gamma-Ca)*J+2.0*(Ca+2.3*Gamma)*Rd;
            cAj= Math.pow(0.2*J-Rd,2);
            dAj= Math.sqrt(aAj*gnoon*gnoon+bAj*gnoon+cAj);


            Aj=(0.635/gnoon)*( Math.sqrt(aAj)*Math.pow(gnoon,2.0)/2.0
              + Math.sqrt(cAj)*gnoon  - ((2.0*aAj*gnoon+bAj)/(4.0*aAj))*dAj
              + bAj*Math.sqrt(cAj)/(4.0*aAj)
              + (Math.pow(bAj,2.0)- 4.0*aAj*cAj)/(8.0*Math.pow(aAj,1.5))
              * Math.log( (2.0*aAj*gnoon+bAj+2.0*Math.sqrt(aAj)*dAj)  /(bAj+2.0*Math.sqrt(aAj)*Math.sqrt(cAj)) ) );

//              System.out.println(gs + " "+ Ac + " "+ Aj);
//              Aj=Math.max(Aj,0.0);
//              Ac=Math.max(Ac,0.0);
            this.Ax=Math.min(Ac, Ac);

            Aday=Math.pow(10, -6)*(aday.Length)*Ax*LAI;  // [mol C m-2 d-1]


            rv= Math.pow(gbl*(gs+gcu)/(gbl+gs+gcu),-1.0);


            double air_dens =  1.204;             //(kg m-3)
            double cp = 1013.0;                  //(J kg-1 C-1)
            double sboltz = 5.6697*Math.pow(10,-8);//(W m-2 C-4)
            double l_vap= 2.45*Math.pow(10,6);     //(J kg-1) latent heat vaporation of water

            rr = air_dens*cp/(4.0*sboltz*Math.pow(aday.Tm+273.15,3));
            rc = rh*rr/(rh+rr);

            double SF=2.0; // shape factor converts from projected to total SLA;

            ET_day_mm =
((Math.pow(10,6)*aday.Sdiff/aday.Length)+air_dens*cp*aday.VPDa/rc)/(aday.Press_pa*cp*rv/(0.6219*l_vap*rc +
1000.0*aday.sigma) )*(aday.Length*SF*LAI/l_vap);
//              System.out.println(aday.doy + " "+ this.theta+ " "+ ET_day_mm);
        }

      break;
```

References

Bernacchi, C.J., Singsaas, E.L., Pimentel, C., Portis Jr, A.R., Long, S.P., 2001. Improved temperature response functions for models of Rubisco-limited photosynthesis. Plant, Cell & Environment 24, 253–259.

Best, M.J., Pryor, M., Clark, D.B., Rooney, G.G., Essery, R., Ménard, C.B., Edwards, J.M., Hendry, M.A., Porson, A., Gedney, N., others, 2011. The Joint UK Land Environment Simulator (JULES), model description–Part 1: energy and water fluxes. Geoscientific Model Development 4, 677–699.

Boulangeat, I., Philippe, P., Abdulhak, S., Douzet, R., Garraud, L., Lavergne, S., Lavorel, S., Van Es, J., Vittoz, P., Thuiller, W., 2012. Improving plant functional groups for dynamic models of biodiversity: at the crossroads between functional and community ecology. Global change biology 18, 3464–3475.

Chen, J.M., Liu, J., Cihlar, J., Goulden, M.L., 1999. Daily canopy photosynthesis model through temporal and spatial scaling for remote sensing applications. Ecological modelling 124, 99–119.

Clark, D.B., Mercado, L.M., Sitch, S., Jones, C.D., Gedney, N., Best, M.J., Pryor, M., Rooney, G.G., Essery, R.L.H., Blyth, E., others, 2011. The Joint UK Land Environment Simulator (JULES), model description–Part 2: carbon fluxes and vegetation dynamics. Geoscientific Model Development 4, 701–722.

Farquhar, G.D., von Caemmerer, S. von, Berry, J.A., 1980. A biochemical model of photosynthetic CO2 assimilation in leaves of C3 species. Planta 149, 78–90.

Fyllas, N.M., Gloor, E., Mercado, L.M., Sitch, S., Quesada, C.A., Domingues, T.F., Galbraith, D.R., Torre-Lezama, A., Vilanova, E., Ramírez-Angulo, H., Higuchi, N., Neill, D.A., Silveira, M., Ferreira, L., Aymard C., G.A., Malhi, Y., Phillips, O.L., Lloyd, J., 2014. Analysing Amazonian forest productivity using a new individual and trait-based model (TFS v.1). Geosci. Model Dev. 7, 1251–1269. doi:10.5194/gmd-7-1251-2014

Lavorel, S., Diaz, S., Cornelissen, J.H.C., Garnier, E., Harrison, S.P., McIntyre, S., Pausa, J.G., Perez-Harguindeguy, N., Roumet, C., Urcelay, C., 2007. Plant Functional Types: Are We Getting Any Closer to the Holy Grail? Presented at the Springer.

Medlyn, B.E., Duursma, R.A., Eamus, D., Ellsworth, D.S., Prentice, I.C., Barton, C.V., Crous, K.Y., de Angelis, P., Freeman, M., Wingate, L., 2011. Reconciling the optimal and empirical approaches to modelling stomatal conductance. Global Change Biology 17, 2134–2144.

Reich, P.B., 2014. The world-wide "fast–slow" plant economics spectrum: a traits manifesto. J Ecol 102, 275–301. doi:10.1111/1365-2745.12211

Walker, A.P., Beckerman, A.P., Gu, L., Kattge, J., Cernusak, L.A., Domingues, T.F., Scales, J.C., Wohlfahrt, G., Wullschleger, S.D., Woodward, F.I., 2014. The relationship of leaf photosynthetic traits–Vcmax and Jmax–to leaf nitrogen, leaf phosphorus, and specific leaf area: a meta-analysis and modeling study. Ecology and evolution 4, 3218–3235.